

Dielectric properties of MgO-doped compositionally graded multilayer barium strontium titanate films

M. W. Cole,^{1,a)} E. Ngo,¹ S. Hirsch,¹ M. B. Okatan,² and S. P. Alpay^{2,b)}

¹*U. S. Army Research Laboratory, Weapons and Materials Research Directorate, Aberdeen Proving Ground, Maryland 21005, USA*

²*Materials Science and Engineering Program, CMBE Department, Institute of Materials Science, University of Connecticut, Storrs, Connecticut 06269, USA*

(Received 12 December 2007; accepted 26 January 2008; published online 20 February 2008)

We have grown 5 mol % MgO-doped multilayered $\text{Ba}_{1-x}\text{Sr}_x\text{TiO}_3$ (BST) films having a nominal thickness of 220 nm with compositions of each layer as BST60/40, BST75/25, and BST90/10 (upgraded). We also fabricated undoped upgraded BST and uniform BST60/40 films for comparison. Results show that Mg-doping improves dielectric loss ($\tan \delta=0.008$) and yields better surface roughness (~ 3.1 nm) compared to undoped upgraded BST. Mg-doped films displayed excellent temperature stability with temperature coefficient of capacitances of -0.94 and 1.14 ppt/ $^\circ\text{C}$ from 20 to 90 $^\circ\text{C}$ and 20 to -10 $^\circ\text{C}$, respectively. Mg doping resulted in a moderate dielectric tunability (29%) compared to undoped BST (65.5%) at 444 kV/cm. © 2008 American Institute of Physics. [DOI: 10.1063/1.2870079]

In recent years, much attention has been devoted to the development of tunable dielectric materials for voltage-controlled, frequency-agile phase shifters and filters operating in the microwave regime.¹⁻⁴ Ferroelectrics (FEs) such as barium strontium titanate [$\text{Ba}_{1-x}\text{Sr}_x\text{TiO}_3$ (BST)] have emerged as leading candidates for such applications due to their highly nonlinear dielectric response to an applied electric field, especially in the vicinity of the paraelectric-to-ferroelectric phase transformation temperature T_C .⁵⁻¹⁰ The major challenge in designing material systems for tunable devices is the simultaneous requirement of high tunability ($>40\%$) over a large temperature interval (-20 – $+85$ $^\circ\text{C}$) coupled with low dielectric losses (between 3.0 and 4.0 dB in operational bandwidths ranging from several hundreds of megahertz up to 30 or more gigahertz). We have recently shown that BST multilayer heterostructures consisting of three distinct layers of ~ 220 nm nominal thickness with compositions corresponding to $\text{Ba}_{0.6}\text{Sr}_{0.4}\text{TiO}_3$ (BST 60/40), BST 80/20, and BST 90/10 on Pt-coated Si substrates have a small-signal dielectric permittivity of 360 with a dissipation factor of 0.012 and a dielectric tunability of 65% at 444 kV/cm.^{11,12} More importantly, these properties were found to exhibit minimal dispersion as a function of temperature ranging from -10 to 90 $^\circ\text{C}$. These results are in accordance with the findings of thermodynamic models that incorporate electrical, mechanical, and electromechanical interactions between BST layers.^{12,13}

Doping of BST with MgO has been identified as one of the ways to reduce dielectric losses in monolithic BST films especially with low strontium content, although the addition of MgO causes a reduction in dielectric response and its tunability.^{14,15} For example,¹⁵ dielectric constant, loss tangent, and tunability (at 237 kV/cm) of BST 60/40 and 5 mol % MgO doped BST 60/40 thin films were reported as 720, 0.1, and 28% and 334, 0.007, and 17.2%, respectively. Thus, acceptor doping combined with compositional grading of BST presents an intriguing opportunity to develop mate-

rials for tunable device applications with stringent demands focused on low dielectric losses and temperature insensitivity, while still maintaining moderate tunabilities. In this letter, we present an experimental study on the effect of MgO addition on dielectric properties of multilayered BST thin films and show that such material systems may indeed be utilized in tunable filters for mobile communication applications such as cellular phones and handheld radios.

BST thin films were grown via metal organic solution deposition (MOSD) on Pt-coated Si substrates. Required amounts of barium acetate, strontium acetate, and titanium (IV) isopropoxide were mixed to prepare the precursor solutions with desired stoichiometry for the BST films. Magnesium acetate was used as a source of Mg. Glacial acetic acid and 2-methoxyethanol were used as solvents. The viscosity and surface tension were adjusted by varying the 2-methoxyethanol content. A detailed description of the MOSD precursor solution preparation and film deposition technique were reported elsewhere.^{16,17} The multilayered thin film design consisted of three distinct compositional layers of ~ 220 nm total thickness with compositions corresponding to BST60/40, BST75/25, and BST90/10. These layers were sequentially deposited onto the Pt-coated Si substrates. A schematic drawing of the thin film multilayered material design is shown in Fig. 1(a). Multilayered film fabrication consisted of depositing three coats of each layer composition onto the substrate, whereby after each individual spin-on film coating, the sample was pyrolyzed at 350 $^\circ\text{C}$ for 10 min and, subsequently, postdeposition annealed at 750 $^\circ\text{C}$ for 1 h in flowing O_2 . Thus, each distinct layer composition was fully crystallized prior to the deposition of next compositional layer. For comparison, we have also grown undoped graded BST films with same layer compositions using the same synthesis and pyrolysis/annealing procedures. Furthermore, monolithic BST60/40 films were also deposited. These were subjected to one time annealing at 750 $^\circ\text{C}$ for 1 h in flowing O_2 after a pyrolyzing step at 350 $^\circ\text{C}$ for 10 min.

The crystal structure and surface morphology of the films were determined via glancing angle x-ray diffraction (XRD) and atomic force microscopy (AFM). A Hitachi

^{a)}Electronic mail: mcole@arl.army.mil.

^{b)}Author to whom correspondence should be addressed. Electronic mail: p.alpay@ims.uconn.edu.

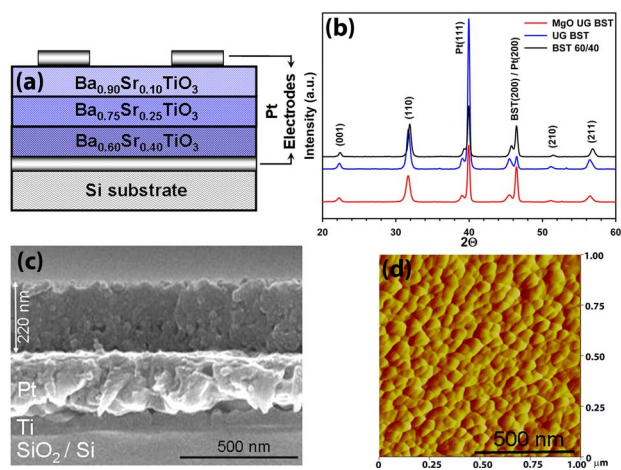


FIG. 1. (Color online) (a) Schematic configuration of multilayered heterostructure BST thin film sandwiched between metallic electrodes. (b) XRD patterns of MgO-doped multilayered, undoped multilayered, and uniform BST thin films. (c) FESEM cross-sectional image of MgO-doped multilayered BST thin film. (d) AFM micrograph showing the plane-view surface morphology of the MgO-doped multilayered BST thin film.

S4500 field emission scanning electron microscope (FESEM) was utilized to assess the cross-sectional microstructure. Rutherford backscattering spectroscopy (RBS) was performed on multilayered films to obtain information on the nature of interfaces between each layer and their composition. The film capacitance and dielectric loss tangent were measured with an HP 4194A impedance/gain phase analyzer. The temperature dependence of dielectric properties was determined using a custom built temperature measurement apparatus and a temperature control box attached to an HP 4194A impedance analyzer.

XRD patterns, as shown in Fig. 1(b), reveal that all of the samples prepared were polycrystalline and single phase, indicating that MgO was fully dissolved in BST perovskite lattice. Compared to bulk BST examined by Su and Button,¹⁸ thin film samples produced in this study displayed an enhanced degree of MgO solubility which can be attributed to a higher degree of chemical homogeneity due to the synthesis method and thermal strains.¹⁹ It was observed that (110) peak of multilayered BST film was shifted to lower angles and also was broader than that of uniform BST60/40. Shifting to lower angles, i.e., an increase in lattice spacing, can be attributed to the increase in molar fraction of Ba⁺² cations, as Ba⁺² cations with an ionic radius of 1.61 Å substitute into the lattice position of smaller Sr⁺² cations having an ionic radius of 1.44 Å.²⁰ Because (110) peak of multilayered BST film is a combination of diffraction from each individual layer of different compositions, it should obviously have a larger full width at half maximum (FWHM) value than the uniform BST film. A further increase in lattice parameter was observed upon MgO doping of multilayered BST film. It is known that Mg⁺² with an ionic radius of 0.72 Å occupies Ti⁺⁴ (ionic radius 0.61 Å) sites which causes the perovskite lattice to expand.²⁰ This deformation of the crystal lattice may also induce elastic strains that may result in a further broadening of the XRD peaks. FWHM values calculated from (110) peak of doped and undoped multilayered thin films were 0.582° and 0.522°, respectively. The lattice parameters of doped, undoped, and uniform BST films were determined as 3.9897, 3.9875, and 3.964 Å, respectively, from their (110) peaks.

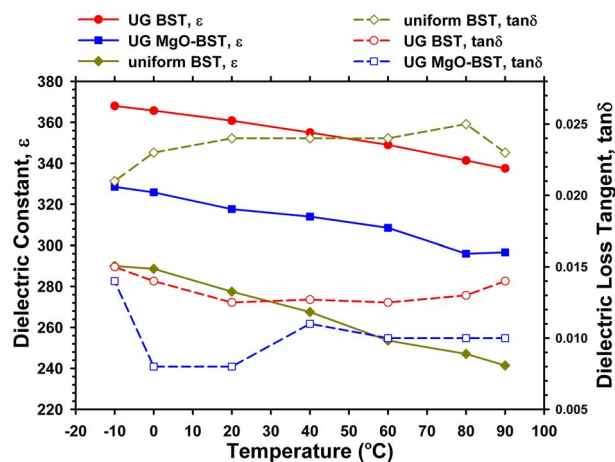


FIG. 2. (Color online) Temperature dependence of dielectric constant and dielectric loss tangent of MgO-doped multilayered, undoped multilayered, and uniform BST thin films.

FESEM images [Fig. 1(c)] taken from the fractured cross section of the MgO-doped multilayered BST films reveal that the films are dense, crack-free, and the substrate/film contact is well-developed, i.e., it is free from voids, amorphous material, and secondary phases. In multilayered samples, no structural delineation was visible under FESEM between each layer. RBS analysis confirmed that no interdiffusion had occurred between these layers during annealing steps so that multilayered thin films were made up of compositionally distinct layers.¹¹ From AFM analysis [Fig. 1(d)], average grain size of undoped and doped multilayered samples were estimated as 72 and 60 nm, respectively, in agreement with FWHM values. Surface roughness of doped films (3.101 nm) was less than that of undoped films (3.479 nm), which is in accordance with smaller grain size of doped films. Low surface roughness ensures an intimate contact between thin film and substrate in device applications. Furthermore, no cracks, surface defects, or pinholes were observed.

Temperature dependence of dielectric constant and loss tangent of thin films are shown in Fig. 2. At a constant temperature, a higher dielectric constant was measured for both doped and undoped multilayered thin films than the uniform BST60/40 film. This can be attributed mostly to the BST75/25 layer for which T_C is close to room temperature and, thus, has a significantly higher dielectric response in monolithic form. Su and Button observed that the dielectric constant was somewhat lowered upon MgO doping which also resulted in a decrease in the ferroelectric transition temperature T_C .¹⁸ These findings, together with the volumetric expansion with the addition of MgO to BST in our films, seem to suggest an effective suppression of ferroelectricity with increased MgO doping due to the substitution of Ti (the displacement of which results in a permanent dipole and, thus, ferroelectric behavior) in the perovskite lattice with Mg cations. Temperature coefficient of capacitance (TCC) was evaluated as the variation of capacitance with temperature relative to the capacitance value at 20 °C. Both MgO-doped and undoped multilayered BST films exhibited a lower dielectric dispersion in the range of -10 to 90 °C than monolithic BST60/40 thin films. As the temperature was elevated from 20 to 90 °C, 6.6% (TCC=-0.94 ppt/°C), 6.4% (TCC=-0.92 ppt/°C), and 13% (TCC=-1.8 ppt/°C) de-

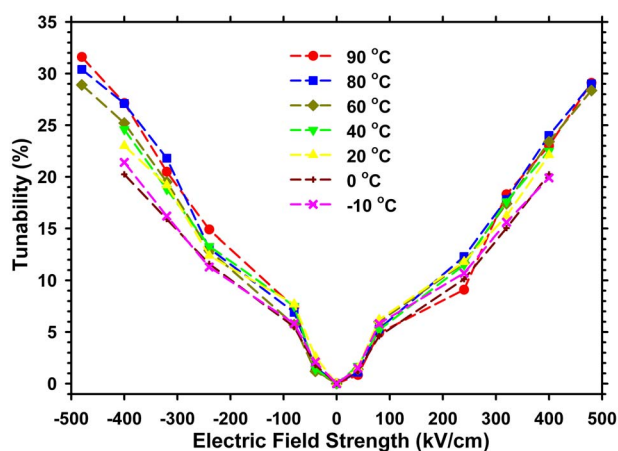


FIG. 3. (Color online) Variation of tunability of MgO-doped multilayered BST thin film at various temperatures.

crease in permittivity was observed for doped multilayered, undoped multilayered, and monolithic BST films, respectively. In the case of lowering temperature from 20 to $-10\text{ }^{\circ}\text{C}$, 3.4% (TCC=1.14 ppt/ $^{\circ}\text{C}$), 2% (TCC=0.67 ppt/ $^{\circ}\text{C}$), and 4.5% (TCC=1.5 ppt/ $^{\circ}\text{C}$) increase in permittivity were noticed for doped multilayered, undoped multilayered, and monolithic BST films, respectively. Additionally, dielectric loss tangent of MgO-doped films was the lowest one among the samples produced in this study. From Fig. 2, it can be seen that, on the average, dielectric loss tangents were 0.009, 0.013, and 0.024 for doped multilayered, undoped multilayered, and uniform BST 60/40 thin films, respectively. A fairly “flat,” i.e., temperature insensitive, and low loss tangent makes it possible for such MgO-doped multilayered BST films to be employed in tunable devices operating over a broad temperature range.

The variation of tunability in MgO-doped BST films at various temperatures is given in Fig. 3. A slight increase in tunability was observed with increasing temperature. At low electric field strengths, i.e., around 250 kV/cm, dispersion in tunability with temperature was quite negligible. However, the tunability of doped multilayered films was lower than both undoped and uniform BST thin films reported earlier.¹¹ For example, at room temperature and at electric field strength of 444 kV/cm, tunability was measured as 65.5%, 42%, and 29% for undoped upgraded, uniform, and doped upgraded BST films, respectively.

Our results show that tailoring thin film material design and composition in BST is a promising tool to achieve desired material properties required for specific tunable device applications. For example, for phase shifters, one would re-

quire a large tunability. In this case, undoped multilayered or compositionally graded BST films would be an appropriate choice. On the other hand, for frequency-agile filters operating in the microwave regime, low dielectric losses are a premium. Therefore, acceptor doping combined with compositional grading would yield significantly better loss properties with a reasonable dielectric tunability. Our findings indicate that Mg-doped multilayer BST films are promising materials for such tunable device applications which advocate stringent demands of reduced dielectric loss and temperature stability while maintaining moderate tunability.

The work at UConn was supported by the U.S. Army Research Office through Grant No. W911NF-05-1-0528. The authors would like to thank G. Martin and C. Hubbard for the XRD data collection.

- ¹A. K. Tagantsev, V. O. Sherman, K. F. Astafiev, J. Venkatesh, and N. Setter, *J. Electroceram.* **11**, 5 (2003).
- ²V. O. Sherman, A. K. Tagantsev, N. Setter, D. Iddles, and T. Price, *J. Appl. Phys.* **99**, 074104 (2006).
- ³F. A. Miranda, F. W. Van Keuls, R. R. Romanofsky, C. H. Mueller, S. Alterovitz, and G. Subramanyam, *Integr. Ferroelectr.* **42**, 131 (2002).
- ⁴F. A. Miranda, G. Subramanyam, F. W. van Keuls, R. R. Romanofsky, J. D. Warner, and C. H. Mueller, *IEEE Trans. Microwave Theory Tech.* **48**, 1181 (2000).
- ⁵J. L. Davis and L. G. Rubin, *J. Appl. Phys.* **24**, 1194 (1953).
- ⁶J. Bellotti, E. K. Akdogan, A. Safari, W. Chang, and S. Kirchoefer, *Integr. Ferroelectr.* **49**, 113 (2002).
- ⁷Z. Yuan, Y. Lin, J. Weaver, X. Chen, C. L. Chen, G. Subramanyam, J. C. Jiang, and E. I. Meletis, *Appl. Phys. Lett.* **87**, 152901 (2005).
- ⁸M. Y. El-Naggar, K. Dayal, D. G. Goodwin, and K. Bhattacharya, *J. Appl. Phys.* **100**, 114115 (2006).
- ⁹O. Auciello, S. Saha, D. Y. Kaufman, S. K. Streiffer, W. Fan, B. Kabius, J. Im, and P. Baumann, *J. Electroceram.* **12**, 119 (2004).
- ¹⁰N. K. Pervez, P. J. Hansen, and R. A. York, *Appl. Phys. Lett.* **85**, 4451 (2004).
- ¹¹M. W. Cole, E. Ngo, S. Hirsch, J. D. Demaree, S. Zhong, and S. P. Alpay, *J. Appl. Phys.* **102**, 034104 (2007).
- ¹²S. Zhong, S. P. Alpay, M. W. Cole, E. Ngo, S. Hirsch, and J. D. Demaree, *Appl. Phys. Lett.* **90**, 092901 (2007).
- ¹³Z. G. Ban, S. P. Alpay, and J. V. Mantese, *Integr. Ferroelectr.* **58**, 1281 (2003).
- ¹⁴L. C. Sengupta and S. Sengupta, *Mater. Res. Innovations* **2**, 278 (1999).
- ¹⁵M. W. Cole, W. D. Nothwang, C. Hubbard, E. Ngo, and M. Ervin, *J. Appl. Phys.* **93**, 9218 (2003).
- ¹⁶M. W. Cole, P. C. Joshi, M. H. Ervin, M. C. Wood, and R. L. Pfeffer, *Thin Solid Films* **374**, 34 (2000).
- ¹⁷M. W. Cole, C. Hubbard, E. Ngo, M. Ervin, M. Wood, and R. G. Geyer, *J. Appl. Phys.* **92**, 475 (2002).
- ¹⁸B. Su and T. W. Button, *J. Appl. Phys.* **95**, 1382 (2004).
- ¹⁹O. Okhay, A. Wu, and P. M. Vilarinho, *J. Eur. Ceram. Soc.* **25**, 3079 (2005).
- ²⁰Ionic Radii in Crystals in *CRC Handbook of Chemistry and Physics*, 88th ed. (Internet Version 2008), edited by D. L. Lide (CRC/Taylor and Francis, Boca Raton, FL).